STRETCH ACTIVATION OF A K⁺ CHANNEL IN MOLLUSCAN HEART CELLS

By WADE J. SIGURDSON, CATHERINE E. MORRIS*

Department of Biology, University of Ottawa, Ottawa, Ontario K1N 6N5, Canada

BORYS L. BREZDEN AND DAVID R. GARDNER

Department of Biology, Carleton University, Ottawa, Ontario K1S 5B6, Canada

SUMMARY

Heart ventricle cells of *Lymnaea stagnalis* contain a stretch-activated K⁺ channel which exhibits two open states and three closed states. Over the range 0 to −25 mmHg (1 mmHg = 133·3 Pa), the probability that the channel is open is a steeply non-linear function of negative pressure. Pressure-dependent decreases in the mean times of the longest component of the closed-time distribution are observed in the same range and (because other mean times show no consistent or sufficiently large changes with pressure) are assumed to account for increases in the probability of being open. Channel activity characteristically occurs as bursts with a mean time of 3·6 ms. These bursts contain, on average, 1·7 closings; 78 % of the burst time is spent in the open state. It is concluded that the stretch-sensitive kinetic component is an interburst closed state.

INTRODUCTION

Ventricular muscle cells of *Lymnaea stagnalis* heart, like many cell types, exhibit a resting permeability to K⁺ (Brezden & Gardner, 1984). The most prominent type of activity observed while making single-channel recordings from these cells under near physiological conditions (i.e. normal saline in the bath and in the recording pipette, cell-attached configuration) is that of a K⁺-selective channel sensitive to membrane stretch (Brezden, Gardner & Morris, 1986). Though stretch-sensitive, this channel is not totally quiescent in the absence of applied stretch; adjustments of the pipette ionic conditions (to produce a driving force for K⁺ currents) provide evidence that the channel has a low level of spontaneous activity at the resting potential. Our principal interest in this channel, however, stems not from its possible contribution to the resting potential, but from its sensitivity to membrane stretch.

A different class of stretch-activated channels – ones which discriminate poorly between K⁺ and Na⁺ – has been observed in a number of vertebrate preparations

---

* To whom reprint requests should be sent.

(Guharay & Sachs, 1984; Brehm, Kidokoro & Moody-Corbett, 1984; Cooper, Tang, Rae & Eisenberg, 1986). Of these, that which occurs in embryonic chick skeletal muscle has been most fully characterized (Guharay & Sachs, 1984, 1985). No physiological function has yet been ascribed to these channels but it has been noted that there are similarities in the properties of the channels and those of the mechanosensory membrane of vertebrate hair cells (Sachs, 1986; Hudspeth, 1983).

In only one preparation other than *Lymnaea* cells has the stretch sensitivity of a K^+ channel been specifically tested. Guharay & Sachs (1984) reported that gating of the Ca^{2+}-activated K^+ channel of embryonic chick muscle is unaffected by membrane stretch. Also, in cell-attached patches of frog erythrocytes, a Ca^{2+}-insensitive K^+ channel has been observed which is activated during osmotically induced swelling (Hamill, 1983). There is no evidence to indicate whether membrane stretch *per se* was the activator, or whether some secondary factor, such as a change in intracellular pH, was responsible. Whatever the direct causal agent, it is reasonable to speculate that the swelling-associated activation of gating is related to cell volume regulation. There exists a considerable body of evidence (most of it non-electrophysiological) for volume-induced changes in K^+ permeability (Gilles, 1983; Grinstein, Rothstein, Sarkadi & Gelfand, 1984; Treherne, 1980). The effect of the increased ion permeability is to augment the efflux of intracellular osmolytes. Stretch-induced activation of ion channels could, thus, prevent cell rupture in the face of acute hypo-osmotic stress.

We do not yet know if *Lymnaea* stretch-activated K^+ (SAK) channels function in volume regulation, but the possibility deserves investigation. The aim of this paper is to begin characterizing the effect of membrane stretch on SAK channel gating.

MATERIALS AND METHODS

Cells were prepared for patch recording using the enzymic dispersion technique described previously (Brezden *et al.* 1986). Briefly, pieces of ventricle were treated in 0·25% trypsin (Sigma, type XII-S) for 30 min, followed by 0·1% collagenase (Sigma, type II-S) for 1–2 h. After centrifugation, cells were resuspended in normal saline (see Table 1 for a list of salines) supplemented with glucose and antibiotics.

Patch electrodes were made from Corning 7052 glass (1·6 mm o.d. and either 1·15 mm or 0·80 mm i.d.) and coated with Sylgard 184 (Dow Corning) prior to fire polishing. The suction port of the pipette holder was connected to a mercury

Table 1. *Composition of salines*

	KCl	NaCl	CaCl2	MgCl2	Hepes	EGTA
Normal saline	1·6	50·0	3·5	2·0	5·0	0
30 mmol l⁻¹ K⁺ saline	30·0	50·0	3·5	2·0	5·0	0
Intracellular saline	60	0	0·2	2·0	5·0	2·2

Concentrations given in mmol l⁻¹. The pH was adjusted to 7·6 with concentrated NaOH. For bath solutions, 5 mmol l⁻¹ glucose, 50 i.u. ml⁻¹ pencillin and 50 μg ml⁻¹ streptomycin were added.

manometer with valving to allow either application of negative pressure or equilibration to atmospheric pressure as was appropriate. Recordings were made from cell-attached or inside-out patches using standard techniques (Hamill *et al.* 1981) with List EPC-5 or EPC-7 patch-clamp amplifiers at gains of 50 or $100 \, \text{mV} \, \text{pA}^{-1}$. Data were recorded on analogue tape then digitized for analysis. Experiments were carried out at room temperature (19–25 °C).

Kinetic properties of the channels were analysed in two different ways.

(1) Time-averaged currents were used to gauge the probability of the channels being open as a function of membrane tension. A cursor-driven computer routine was used to establish the zero current baseline and the current level for single-channel openings of the digitized data. If the number of SAK channels in the patch had been known, an absolute value for the probability of being open, P(O), could have been obtained; instead, since the number was not known with certainty, an index of the P(O) is given. This is calculated as the time-averaged current (i.e. the integral of the current divided by the sampling duration) divided by the single-channel current. The largest value of index P(O) (attained at higher pressures) should provide a minimum estimate of the number of channels in the patch. This computerized analysis was limited to data containing sections of zero current baseline. In data obtained at higher pressures such sections were sometimes absent, so index P(O) was obtained by evaluating the current integral from chart recordings of raw data.

(2) For analysis of open and closed times (using records which contained few simultaneous channel openings), the data were filtered at 4 kHz (eight-pole Bessel) prior to digitization at $50 \, \mu\text{s point}^{-1}$. Processing by automatic threshold detection software then yielded event durations which were used for open- and closed-time histograms. The detection threshold was set halfway between the baseline and the open-channel level. Only events which exceeded threshold and persisted for $100 \, \mu\text{s}$ or longer were counted. Time constants were extracted from the data by regression of a sum of exponential probability density functions using, with slight modifications, the Marquardt non-linear least-squares algorithm of Schreiner, Kramer, Krischer & Langsam (1985), run on a Compaq 286 computer. The fitting procedure adopted was essentially that used by Guharay & Sachs (1984): data were compared to the integral over each bin of the appropriate function (i.e. the sum of one, two or three exponentials), with bin widths adjusted to contain a minimum of five counts. The squared residuals were weighted inversely with the expected variance (see equation 39, Colquhoun & Sigworth, 1983). The number of exponential terms to fit our data best was chosen on the basis of a minimum chi-squared value derived from the fitting routine (see Colquhoun & Sigworth, 1983).

Since channel currents tended to occur in short bursts, a burst analysis has also been carried out. When bursts of openings are well separated, the estimate obtained for the average burst duration should be insensitive to the choice of interburst interval (i.e. the minimum duration for a closed event which is deemed to represent a period between bursts) (Colquhoun & Hawkes, 1982). When bursts are closely spaced in the record, it is not known whether a given closed event is a between-bursts

or a within-burst event, so that estimation of burst length is not possible. To provide a criterion for deciding, in the first place, whether data were suitable for burst analysis and for deciding, subsequently, what interburst interval was appropriate, the following procedure was developed. (a) Raw data were processed through the threshold detection program, yielding an idealized sequence of open and closed states. (b) For a series of different interburst intervals, the average burst length, the average proportion of the burst spent in the open state and the average number of closings per burst were calculated from the idealized record. Examination of these parameters plotted against interburst interval formed the basis for an empirical choice of interburst interval (see Fig. 8). (c) A new idealized record was produced in which all closings briefer than the chosen interburst interval were suppressed. The distribution of open and closed times in this record of bursts was then analysed in the manner already described. [For mathematically derived criteria for choosing inter-burst intervals, see Magleby & Pallotta (1982) and Colquhoun & Sakmann (1985).]

RESULTS

SAK channels are stretch-sensitive under a wide range of conditions

SAK channels (Fig. 1A) are not the only type observed in ventricle cell membrane, but other, as yet uncharacterized, types (Fig. 1B–E) are far less evident. The SAK channel can be distinguished from others on the basis of its relative amplitude and its flickery kinetics, but these characteristics vary with membrane potential and ionic conditions. An indispensable characteristic used for SAK channel identification is the increase in activity observed when suction is applied. For quick diagnostic tests of stretch activation, we bypassed the syringe/manometer assembly and used uncalibrated suction.

Stretch activation of the SAK channel was demonstrable under a wide range of conditions. The most nearly physiological condition was that involving cell-attached, single-channel recording with normal saline in the bath and pipette. Under these conditions, SAK channel activity was not apparent at the resting potential (about $-60\,\text{mV}$ for these isolated cells, Brezden *et al.* 1986), but when the driving force was increased by a depolarization of $20\,\text{mV}$ or more, stretch activation of the SAK channel could be detected (e.g. Fig. 2A). Mechanical effects on the gating of the SAK channel are thus not likely to be mere epiphenomena, elicited only under bizarre conditions; there are reasonable prospects that stretch activation of the SAK channel is of physiological significance.

To observe stretch activation of the channel at the resting potential, the K^+ concentration in the pipette was increased (e.g. to $30\,\text{mmol}\,\text{l}^{-1}$). Under these conditions, inward current through the SAK channel was readily resolved at rest. The probability that the channels were open was increased when suction was applied (Fig. 2B).

Although SAK channels were consistently observed on cell-attached patches with normal saline in the pipette, they 'disappeared' when the patch was torn off to give symmetrical normal saline on either side. This disappearance was not an artefact of
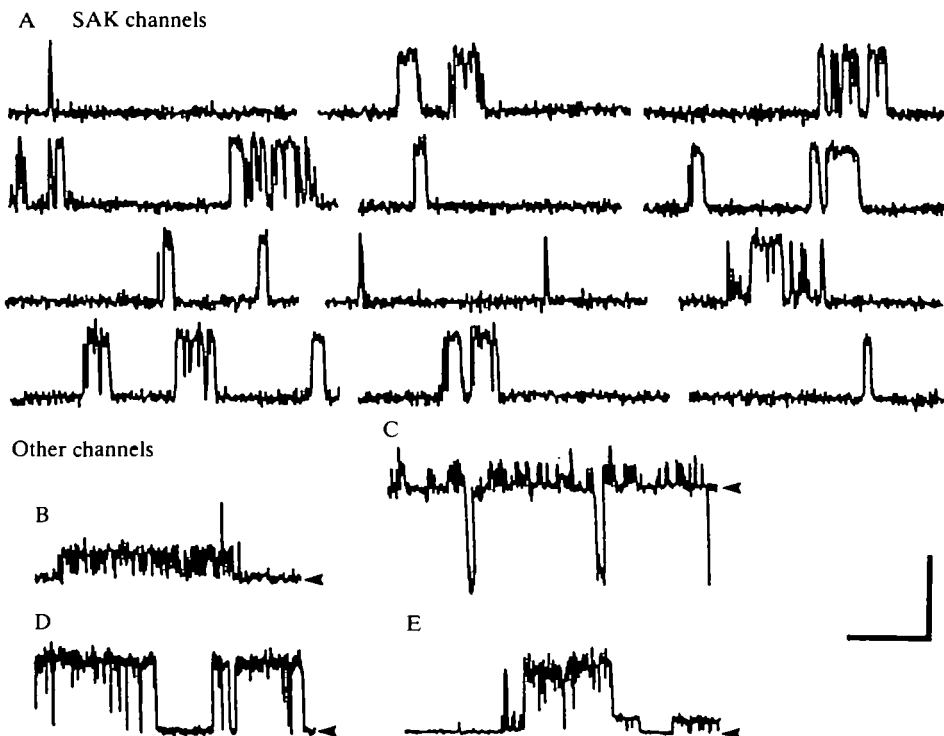
A   SAK channels

Other channels

B

C

D   E

Fig. 1. Single-channel recordings from *Lymnaea* ventricle muscle. (A) SAK channels recorded under cell-attached conditions with 30 mmol l^{-1} K$^+$ saline in the pipette and $V_m = +40$ mV. In this and all subsequent figures, upward deflections from the baseline represent outward membrane current. For purposes of calculating V_m, the resting potential is assumed to be -60 mV (see Brezden, Gardner & Morris, 1986). No pressure was applied for these records. Scales: horizontal, 25 ms; vertical, 2·5 pA. (B) A channel seen in about one-third of the patches. This channel has a smaller conductance than the SAK channel and produces prolonged bursts of outward current under ionic and voltage conditions at which SAK channel current is also outward. The activity of this channel is sporadic but showed no evidence of increasing with applied stretch. Cell-attached patch, 30 mmol l^{-1} K$^+$ saline in the pipette, $V_m = +40$ mV. Horizontal arrowhead indicates position of the zero current baseline. Scales: 5 s, 2·5 pA. (C) SAK channels (small deflections upward from the baseline) and a channel which we surmise must be passing inward Na$^+$ current (there is no driving force on Cl$^-$ and Na$^+$ is the only other ionic species available in the pipette to carry an inward current). Channel activity with these characteristics was only noted in one patch. Inside-out patch, normal saline in the pipette, intracellular saline in the bath, $V_m = 0$ mV. Scales: 250 ms, 2·5 pA. (D) A large, long-lived channel seen in a few inside-out patches when Ca^{2+} was present on the intracellular side. This channel has a conductance of about 100 pS in symmetrical normal saline. It is not known which of the two predominant ion species (Na$^+$ or Cl$^-$) is responsible for this current. $V_m = +70$ mV for this trace. Scales: 5 s, 5 pA. (E) Events recorded in symmetrical normal saline inside-out patch at $V_m = +100$ mV. This channel activity differs from that in D in that a number of open levels are seen. This may correspond to the multiple-conductance Cl$^-$ channel described in *Lymnaea* neurones under similar recording conditions (Geletyuk & Kazachenko, 1985). Scales: 5 s, 25 pA.

vesicle formation at the pipette tip, since other channels were seen (Fig. 1D,E), such as a large (100 pS) channel which may be similar to the Cl$^-$ channel observed in *Lymnaea* neurones (Geletyuk & Kazachenko, 1985). The lack of SAK channel currents under these conditions is most reasonably attributed, therefore, to the reduced level of permeant ion when K$^+$ is present at only 1·6 mmol l^{-1} on both sides.

A variety of K$^+$ channels is activated by low levels of intracellular Ca^{2+} (Latorre & Miller, 1983). Since there is good circumstantial evidence for the existence of mechanically activated Ca^{2+} channels (Eckert, 1972) and since volume-sensitive K$^+$ pathways in many cell types are Ca^{2+}-dependent (Grinstein, Dupre & Rothstein, 1982), there was reason to wonder whether stretch activation of SAK channels is induced indirectly through stretch modulation of Ca^{2+} influxes. We examined this possibility and have the following lines of evidence to indicate that Ca^{2+} is not involved.
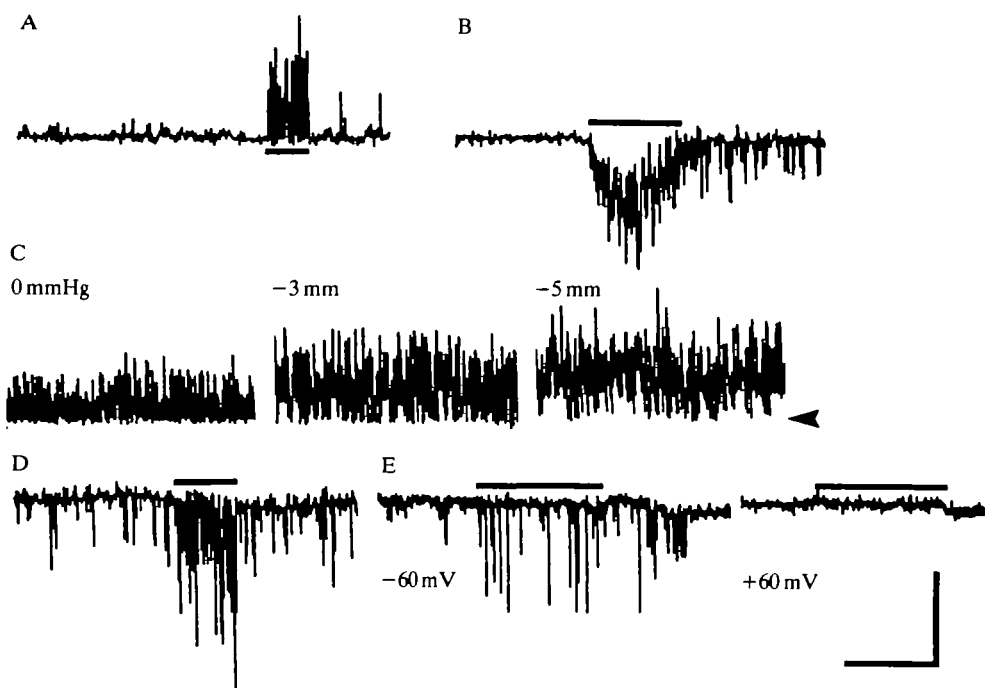

Fig. 2. SAK channels are stretch-sensitive under a wide range of conditions. (A) Cell-attached, normal saline in the pipette, $V_m = -20$ mV. Scales: 5 s, 5 pA. For this trace, as well as B,D and E, application of suction is indicated by the bar. (B) Cell-attached, 30 mmol l^{-1} K$^+$ saline in the pipette, $V_m = +60$ mV. Scales: 5 s, 5 pA. (C) Inside-out patch, normal saline in the pipette, intracellular saline perfused over inner side. The high background (e.g. at 0 mmHg) level of SAK channel activity may be due to pressure exerted by the flowing saline of the perfusion pipette. Channel activity increases when −3 mmHg and −5 mmHg are applied. Scales: 5 s, 5 pA. (D) Cell-attached, intracellular saline in the pipette, $V_m = -60$ mV. Scales: 5s, 2·5 pA. (E) Inside-out, intracellular saline in the pipette, normal saline in the bath, $V_m = -60$ mV or $+60$ mV. Although large outward currents flow through the SAK channel when K$^+$ is the major cation on the inner side of the membrane, it is not possible to force an outward Na$^+$ current through the channel. Scales: 5 s, 2·5 pA.

(1) Under cell-attached conditions (with normal saline or with $30 \, \text{mmol} \, l^{-1} \, K^+$ in the pipette) stretch activation was observed at membrane voltages at which the driving force for Ca^{2+} influx should be minor (i.e. in the range $V_m = +90 \, \text{mV}$).

(2) Using normal saline, inside-out patches were formed. An 'intracellular saline' with $EGTA/Ca^{2+}$ added to give a $[Ca^{2+}]$ of $10^{-8} \, \text{mol} \, l^{-1}$ (Table 1) was then perfused over the inner face of the membrane (using the patch perfusion technique described by Yellen, 1982). Stretch activation of the SAK channel was demonstrable under these conditions (Fig. 2C).

(3) When intracellular saline was used in the pipette with the cell-attached configuration, the SAK channel could be activated by stretch (Fig. 2D). Under these conditions the Ca^{2+} concentration on both sides of the patch of membrane was negligible.

(4) When Ca^{2+} was present at $3 \cdot 5 \, \text{mmol} \, l^{-1}$ on the inner face of the membrane (inside-out patch with intracellular saline in the pipette and normal saline in the bath) stretch activation of the channels was apparent (Fig. 2E). Any Ca^{2+} fluxes occurring during stretch would have no effect on the $[Ca^{2+}]$ at the inner face of the membrane.

In addition to testing the effects of Ca^{2+} on SAK channel stretch sensitivity, we exposed the channels to two drugs which antagonize certain species of Ca^{2+}-activated K^+ channels. Apamin, which blocks Ca^{2+}-activated K^+ channels in cultured rat muscle cells (Hugues *et al.* 1982), and cetiedil, which abolishes the volume-induced, Ca^{2+}-sensitive K^+ pathways in peripheral blood lymphocytes (Sarkadi, Mack & Rothstein, 1984), were applied in the pipette at 10^{-6} and $10^{-5} \, \text{mol} \, l^{-1}$, respectively. Neither drug had any evident effect on SAK channel conductance, kinetics or responsiveness to stretch.

SAK channel conductance is insensitive to membrane tension

Current/voltage (I/V) curves generated for the SAK channel in the presence and the absence of suction were indistinguishable (Fig. 3); we did not observe an increase in channel amplitude during the application of negative pressure. It can, therefore, be concluded that membrane tension does not affect the conformation of that region of the SAK channel which is rate limiting for ion permeation.

Effect of membrane tension on the probability that the channel is open

Once it is established that membrane tension does not alter channel conductance, it can be assumed that changes in the time-averaged current measured at various tensions arise from changes in channel kinetics. This is readily apparent in Fig. 4, which shows single-channel recordings from a patch subjected to a series of increasing negative pressures. The number of multiple openings increases until finally individual events can no longer be resolved. As shown by the change in current when pressure is released from $-25 \, \text{mmHg}$ to $0 \, \text{mmHg}$, stretch activation of SAK channel gating is reversible. This example also illustrates, however, that full relaxation to the initial (0 mmHg) level of activity may require a time of the order of
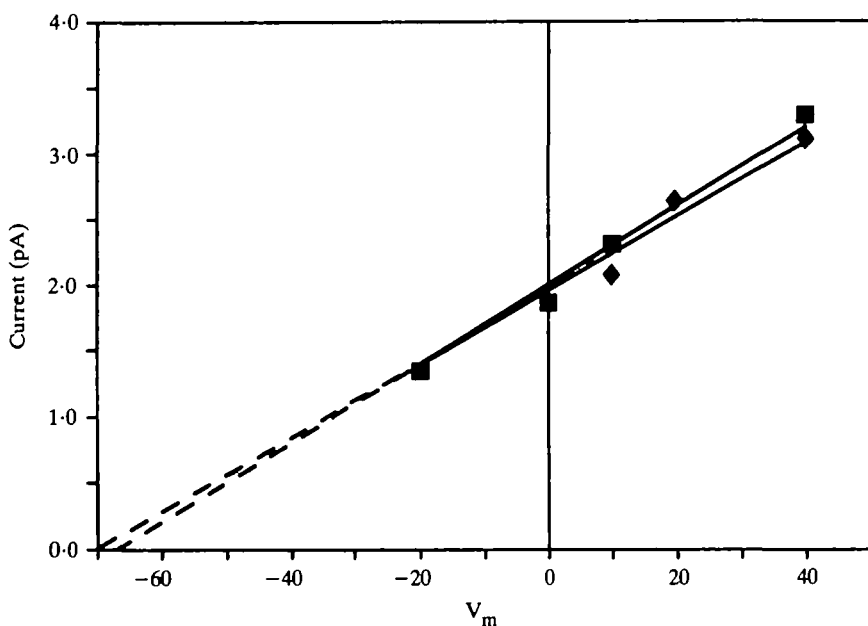
Fig. 3. A comparison of current/voltage relationships for SAK channels without pressure (■) and with −10 mmHg (◆). Data were obtained on a cell-attached patch with normal saline in the pipette. The slope conductance for both regression lines is 33 pS.
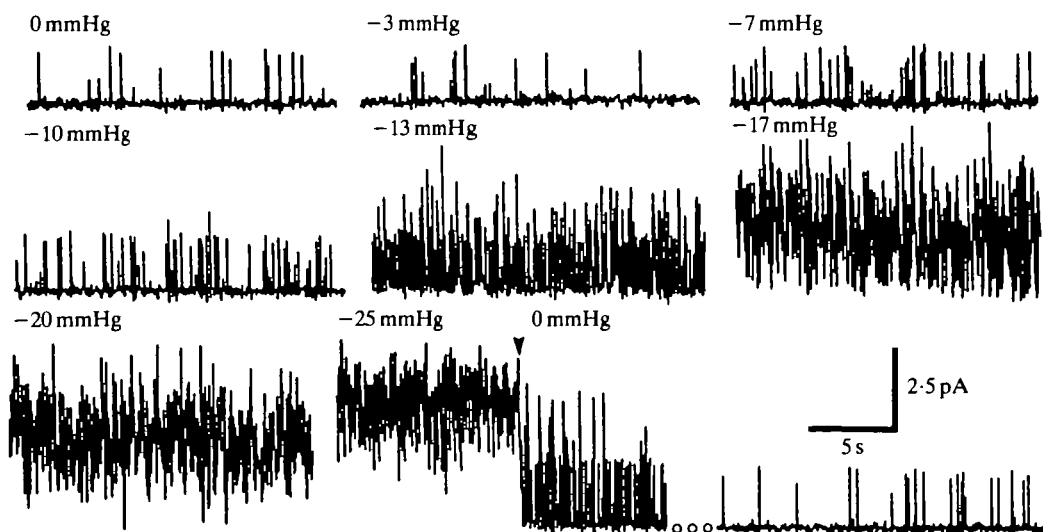

Fig. 4. SAK channel activity at a series of negative pressures. Cell-attached patch, $30 \text{ mmol l}^{-1} \text{ K}^+$ in pipette, $V_m = +140 \text{ mV}$. Arrowhead indicates release of suction. The continuous record at 0 mmHg (following −25 mmHg) is interrupted then continued 85 s after release of suction. (The limited time resolution of the x–y plotter accounts for the apparent variability in channel amplitudes which are, however, of unitary height, as shown in Fig. 1A.)

minutes. Evidently, there are fast and slow aspects to the process; further study of the relaxation dynamics is needed.

Time-averaged currents for such records can be plotted [as an index of the probability of being open, P(O)] against applied pressure (Fig. 5). The position of the stretch activation curve along the pressure axis varied considerably among patches, but in all cases index P(O) is a non-linear function of applied pressure. In the cases in which the patch lasted long enough for a complete pressure series, the curve was sigmoidal. This indicates that, in the range of pressures which the membrane can withstand without breaking, stretch activation can saturate. It can also be noted that, in the region of saturation, the current record (e.g. Fig. 4, −25 mmHg) is very noisy. This is not what would be expected if stretch prolonged open states of the SAK channel. However, a large variance in the current record at saturating pressures is precisely what would be predicted if stretch reduced the duration of a closed state which separates intrinsically flickery bursts of single-channel activity.

It is not clear whether it would be more correct to describe the foot of the P(O) curve as a threshold region or more simply as a region where the effect of stretch is undetectably low. If it is a true threshold, it may be related to the manner in which
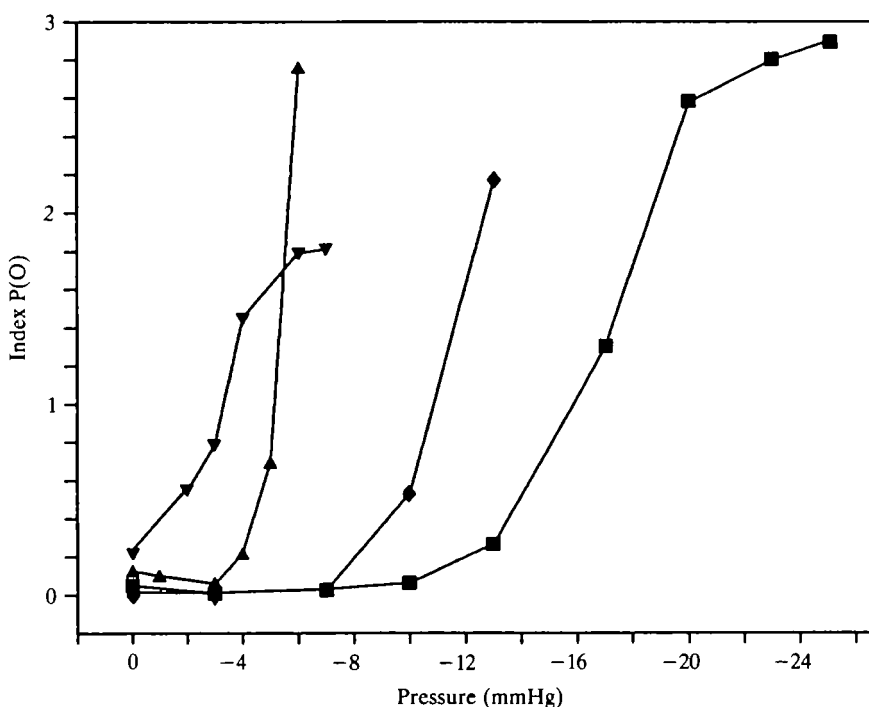

Fig. 5. The effect of negative pressure on the probability that the SAK channel is open for different patches with 30 mmol l^{-1} saline in the pipette. Ordinate: index of P(O), as explained in the text. Abscissa: applied pressure. ▲, cell-attached, $V_m = -80$ mV; ▼, inside-out, normal saline in bath, $V_m = -40$ mV (same patch as ▲); ◆, cell-attached, $V_m = -120$ mV; ■, cell-attached, $V_m = +40$ mV.

pressure affects patch geometry. Using thin-walled glass on excised patches, it was just possible to see (with Nomarski optics at 400×) the patch while pressure was applied. With this glass, the patch formed about 10 μm inside the pipette, where the walls were quite parallel. Below about -5 mmHg, the patch appeared flaccid and irregular; only at higher pressures did it round up and distend. It should be noted that during this distension the patch rim (i.e. the region of the seal) showed no signs of moving.

The observations confirmed that suction does indeed exert mechanical forces on the membrane, but made us reluctant to assume that membrane tension varies in a simple fashion with variations in applied pressure. It would be inappropriate at this stage, therefore, to attempt to quantify the stretch sensitivity of the SAK channel on the basis of equations (see Guharay & Sachs, 1984) which assume a well-defined functional relationship between membrane tension and applied pressure. However, an investigation can be made of how changes in the gating of the SAK channel produce the increased P(O) during application of negative pressure. We have suggested that a closed state is more likely to be affected directly by stretch than an open state. Analysis of open and closed states allows us to test this hypothesis directly.

Open and closed states of the SAK channel

To determine the number of kinetically distinguishable states which the SAK channel can assume, open- and closed-time distributions were analysed. Data containing several thousand transitions and few multiple openings are required. Ideally, one-channel patches would be used for such analyses; in practice, few-channel patches, such as those we were able to obtain, are acceptable. To achieve smaller patches than those used in the P(O) experiments, we used the thicker walled glass with heavily fire-polished tips. The optical distortion from these pipettes was more severe; nevertheless, it was evident that the patch was not forming partway up the shank and so must have formed very near the tip. Variability in the pressure required for activation was also observed with smaller patches. Because P(O) changed so abruptly with increasing negative pressure, it was difficult to obtain complete data sets. Usually data were amenable to kinetic analysis for only part of the pressure range; too few transitions occurred at low pressures whereas too many 'doubles' occurred at pressures only slightly higher. Nevertheless, data were obtained from a number of patches at pressures ranging from 0 to -45 mmHg. Patches were held at a depolarized voltage ($V_m = +30$ to $+60$ mV) and the cell-attached condition was used. Data obtained with normal saline and 30 mmol l^{-1} K$^+$ saline in the pipette are included.

The distribution of open times consistently showed a better fit to a sum of two exponentials than to a single exponential. An example of an open-time histogram is shown in Fig. 6A. For closed times, three exponentials produced the best fits, as illustrated in Fig. 6B. The SAK channel thus has a minimum of five states, two open and three closed.

For a scheme in which the connections between states is known, the mean dwell time in a given state may be written as the reciprocal of the sum of all the rates for leaving that given state. If any of the component rates were stretch-sensitive, this would be reflected in the mean dwell time, or time constant. In Fig. 7A,B the time constants for the distribution of open times, and for the two faster components of the
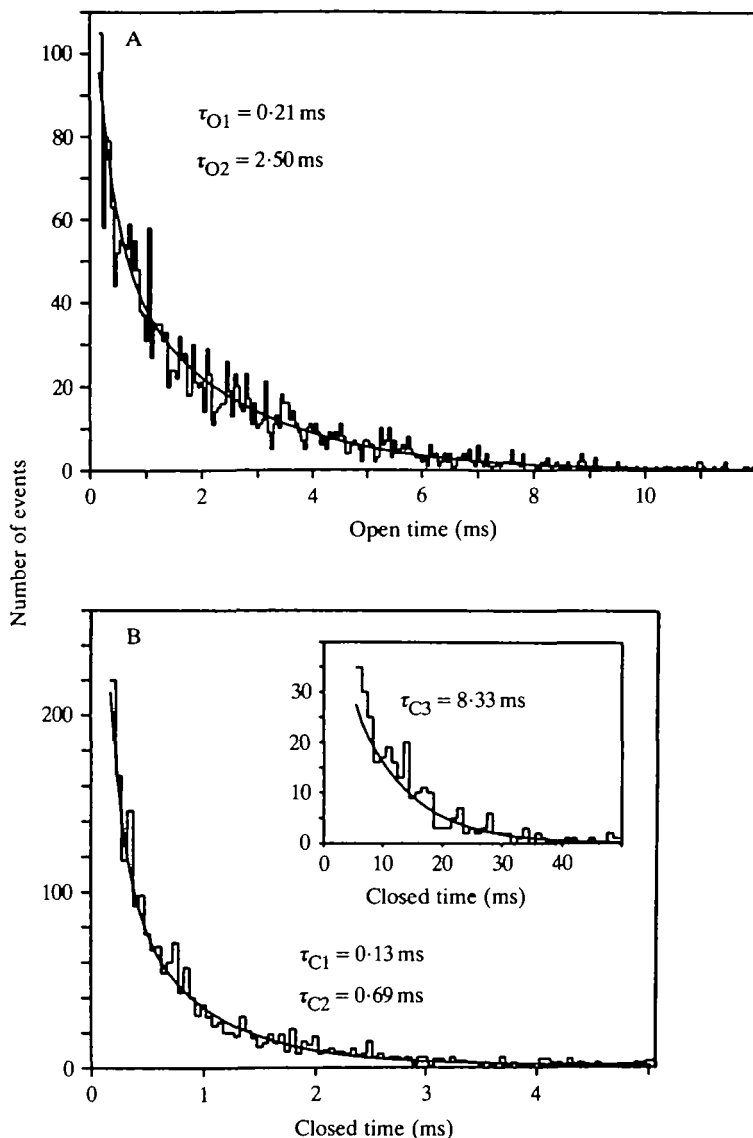

Fig. 6. Open- (A) and closed-time (B) histograms for SAK channels in a cell-attached patch held at -30 mmHg and $V_m = +60$ mV. The time constants associated with the fitted function (continuous line drawn over the histogram bins) are indicated (O, open; C, closed). The tail of the third exponential fitted to the closed times is shown as an inset. Although data were rebinned for the fitting process (see Materials and Methods) they are displayed here with uniform-size bin widths.

distribution of closed times, are plotted as a function of applied pressure. There are no consistent indications that the time constants for these distributions are stretch-sensitive, and certainly there are no changes that could account for the large changes in P(O) as a function of pressure.

By elimination, the only remaining time constant (τ_{C3}) must be stretch-sensitive to account for pressure-induced changes in P(O), and this is supported by the data for this time constant (Fig. 7C).

When several-channel patches were used to evaluate time constants, open times could be obtained unambiguously (provided the frequency of simultaneous openings was low), just as for one-channel patches. Certain of the closed times obtained, however, will be inversely scaled with the number of channels in the patch. Of the three closed times, τ_{C1}, τ_{C2} and τ_{C3}, it is likely that only τ_{C3} is affected in this way. Since data were obtained only from records containing few simultaneous openings,
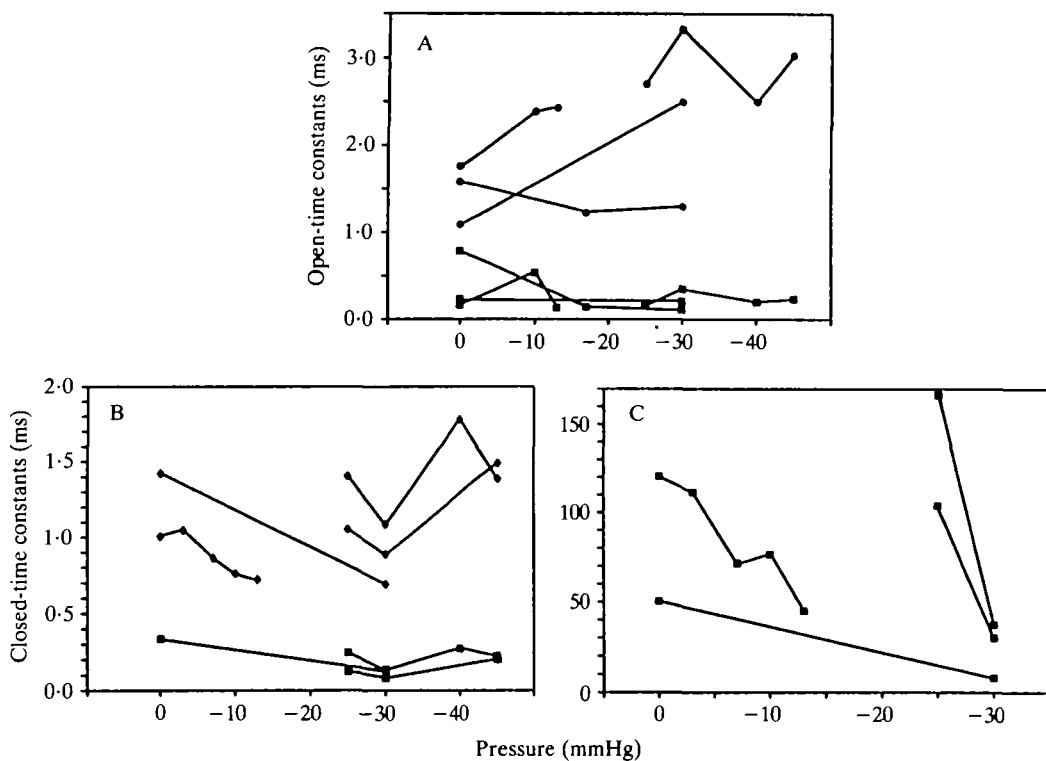

Fig. 7. Time constants extracted from exponential fits as a function of pressure. The points connected by lines represent one cell-attached patch held at a constant potential (+30, +40 or +60 mV). (A) ■ τ_{O1}, ● τ_{O2}; (B) ■ τ_{C1}, ◆ τ_{C2}; (C) τ_{C3}. As explained in the text, the values for τ_{O1}, τ_{O2}, τ_{C1} and τ_{C2} reflect the true time constants, whereas those for τ_{C3} are expected to scale inversely with increasing numbers of channels in the patch, and therefore are expected to vary widely from patch to patch. Inspection of the raw data indicates that τ_{C3} for the two rightmost patches in C continued to increase with decreasing negative pressure, but adequate three-exponential fits to the data could not be obtained because of the low relative density in the tail of the distribution.

and since τ_{C1} and τ_{C2} (as well as τ_{O1} and τ_{O2}) are small compared to τ_{C3}, one can assume that short-lived closures of a given SAK channel will seldom be followed by opening of a different SAK channel. In other words, information on the rate of transitions out of short-lived closed states (like those out of open states) are contributed in a manner that is almost equivalent to having a one-channel patch.

By contrast, when a given channel enters a long-lived closed state, there is a substantial probability that the next opening will be that of a different channel. The open- and closed-time analysis suggests, therefore, that the channel undergoes periods of activity involving excursions among its short-lived open and closed states followed by entry into a longer-lived closed state. When the membrane is not under tension the channel remains in this state for hundreds of ms. With increasing tension, the transition rate(s) for leaving the state increases. There is, on the other hand, no evidence that the rate(s) for entering a long-lived closed state changes with pressure.

SAK channel bursts

A further analysis of the bursting behaviour of the SAK channel has been made using the procedure given in Materials and Methods. In Fig. 8 are plotted the estimated average burst duration, the proportion of time spent in the open state within the burst and the average number of closings per burst for a series of pressures for one patch (Fig. 8A) and three patches with no applied pressure (Fig. 8B). In the burst duration graph of Fig. 8B we also illustrate a result taken at a pressure that produced a frequency of activation too high to allow for burst analysis. On the basis of these graphs, we chose 3 ms as an appropriate interburst interval, since estimates of the parameters should change only slightly for increasing interburst intervals between about 2 and 10 ms. To illustrate this, we did some analyses with a 6 ms interburst interval (Table 2).

The shapes of the curves of Fig. 8 can be explained if one first considers the case of an extremely brief interburst interval: when a sufficiently small interval is chosen, virtually all open events will be regarded as 'bursts'. Consequently, the estimated average burst length will be an arithmetic mean of all open events, the estimated proportion of burst time spent in the open state will approach one, and the estimate for closings per burst will approach zero. As longer intervals are chosen, open states coalesce into bursts; if the true interburst intervals are long compared to other closed states, a region in the curves should appear where there is little change in the parameter estimates. With further increases in the choice of interval, bursts will begin to coalesce and the estimates will again change steeply with the chosen interval. The graphs show that on the time scale we examined, the SAK channel tends to burst, but that the bursts do not occur in detectable clusters (which would have produced a third plateau region in the graph for burst duration). The graphs also indicate that it is reasonable to choose one interburst interval and use it to analyse data for different patches and different pressures. The burst duration curve for −30 mmHg (Fig. 8B) which shows no 'burst plateau' illustrates why further burst analysis cannot be undertaken on all data sets.

The next step, having chosen an interval, is to examine the distribution of burst and interburst durations. A histogram of burst durations is illustrated in Fig. 9; the bursts are best fitted by a sum of two exponentials (Table 2). The faster of the two components is small, constituting about 10–15% of the total number of events, but its inclusion in the estimates of burst parameters effectively 'contaminates' assessment of the dominant burst component. To eliminate the faster component, we
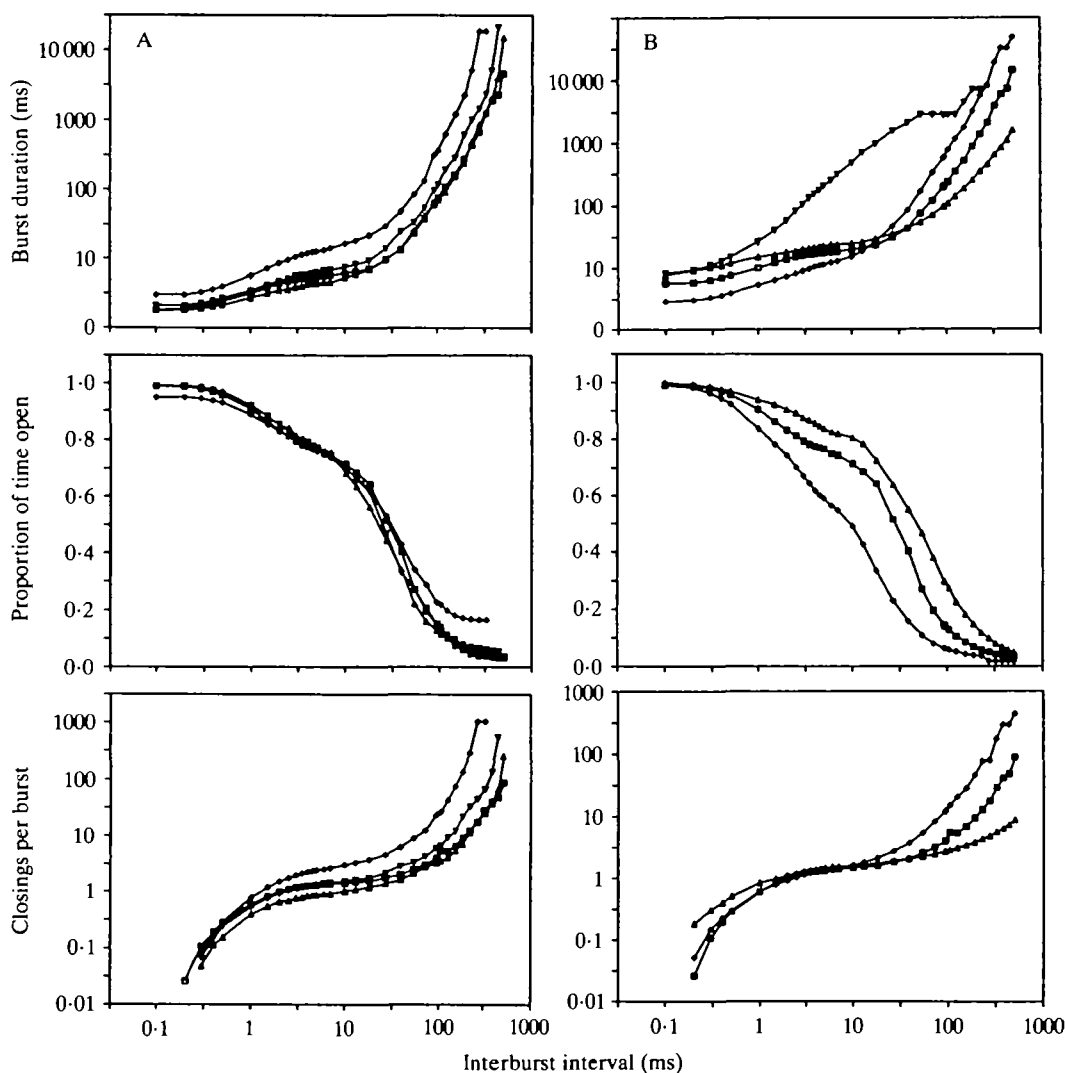

Fig. 8. Determination of burst parameters using different interburst intervals as explained in the text. (A) Data obtained from the same patch at four pressures, ■ 0 mmHg, ▲ −7 mmHg, ▼ −10 mmHg and ◆ −13 mmHg (patch 1 of Table 2). (B) Data obtained at 0 mmHg for three different patches (■ 0 mmHg from A, ▲ patch 3 of Table 2, ◆ patch 2 of Table 2) plus burst duration data (▼) for the same patch as ◆ but at −30 mmHg. Note that abscissae are logarithmic, as are the ordinates for burst duration and closing per burst.

Table 2. *Burst kinetics*

Parameter	0 mmHg	Applied pressure		
		−7 mmHg	−10 mmHg	−13 mmHg
Patch 1				
Index P(O)	0·04	0·03	0·06	0·27
$\tau_{burst/fast}$ (ms)	0·20	0·44	0·39	0·20
$\tau_{burst/slow}$ (ms)	4·7 (4·4)*	4·7 (4·2)	6·0 (6·4)	11·1 (14·9)
$\tau_{interburst}$ (ms)	113·8	111·0	65·8	40·4
τ_{C3} (ms)	120·5	111·4†	77·9	45·5
Closings per burst	1·4	1·0	1·4	2·2
Proportion of time open	0·79	0·81	0·80	0·80

	0 mmHg	0 mmHg
Patches 2 and 3 ·		
$\tau_{burst/fast}$ (ms)	0·14	0·12
$\tau_{burst/slow}$ (ms)	2·6 (3·8)	3·5 (4·2)
$\tau_{interburst}$ (ms)	46·1	397·7
τ_{C3} (ms)	50·0	323·5
Closings per burst‡	1·7	1·9
Proportion of time open	0·66	0·88

* The values in parentheses were obtained using an interburst interval of 6 ms whereas all others are based on a 3 ms interburst interval.

† This value was obtained from a single exponential fit to all closed times ≥5 ms, whereas other τ values are obtained from multiple exponential fits.

‡ Closings per burst pertain to slow bursts only, as explained in the text.

All data are from cell-attached patches. Patch 1, 30 mmol l^{-1} saline in the pipette, V_m = +40 mV; patches 2 and 3, normal saline in the pipette, V_m = +60 and +30 mV.

discarded bursts shorter than 0·7 ms and recalculated the number of closings per burst and the proportion of time spent in the open state (Table 2). For 0 mmHg, the number of closings per burst calculated in this way was 1·66 ± 0·26 (s.d., N = 3) and the proportion of time spent open was 0·78 ± 0·11 (N = 3). The mean burst duration ($\tau_{burst/slow}$, based on an interburst interval of 3 ms) for these data is 3·6 ± 1·1 ms.

The closed intervals between bursts fit well to a single exponential with values corresponding to those of τ_{C3} at the various pressures tested (Table 2).

This method of obtaining burst parameters while simultaneously monitoring the interburst interval (which we take to be the equivalent of τ_{C3}) should simplify future studies of the SAK channel. Applying this approach for more complete series of pressures (in the region where pressure is just beginning to activate the channel) should allow us to determine with more certainty whether pressure affects only the longest-lived closed state.

DISCUSSION

The SAK channel of *Lymnaea* cardiac muscle appears to be at least as stretch-sensitive as the cation channel in chick skeletal muscle described by Guharay & Sachs (1984). Over the range 0 to −50 mmHg, for the chick channel, ln P(O) was a

continuously linear function of the pressure squared; saturation of the function presumably does not occur in this range. For *Lymnaea* SAK channels, the region of steep ascent of the P(O) curve falls well within the −50 mmHg level, and for two patches we were able to show that saturation occurs below −25 mmHg. If the SAK channel is indeed somewhat more stretch-sensitive than the chick muscle channel, this would not necessarily relate to a greater gain in the underlying transduction mechanism of the SAK channel. By pretreating their cells with cytochalasin B,
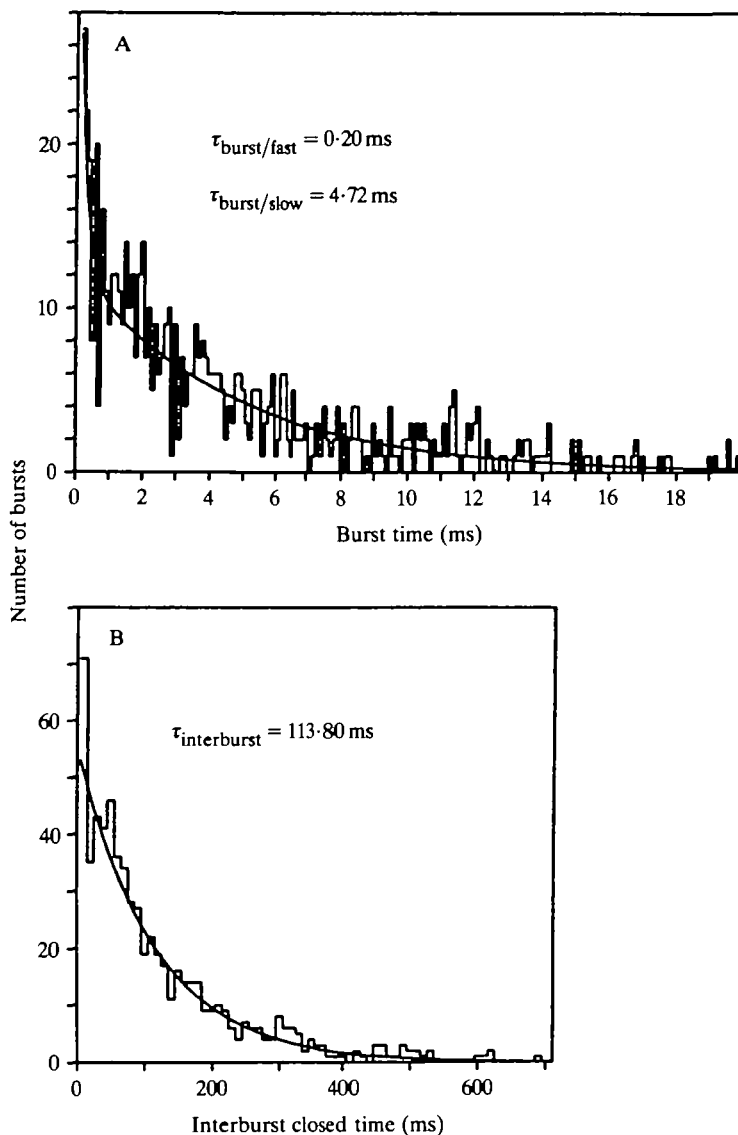

Fig. 9. Histograms for SAK channel burst activity. An interburst interval of 3 ms was used in this example, which is from a cell-attached patch held at 0 mmHg and $V_m = +40$ mV. The burst distribution has been fitted to the sum of two exponentials whereas interburst intervals can be described by a single exponential.

Guharay & Sachs (1984) were able to show that much of the membrane tension is normally relieved by actin-containing elements. The stretch sensitivity of channels from cytochalasin-treated cells was 30 times greater than that of channels from normal cells. It may be that the extent of stretch sensitivity and the inherent variability that we observed for the *Lymnaea* SAK channels reflects the condition of accessory membrane structures in our patch preparations.

The *Lymnaea* SAK channel and the chick channel share a number of kinetic features. Both channels show some spontaneous activity at 0 mmHg. Activity in both channels tends to occur in bursts dominated by the open state. For the SAK channel, the number of closings detected by our analysis procedure (i.e. those which exceeded the halfway threshold and then persisted for at least 100 μs) was 1·7 burst^{-1}. The actual number is undoubtedly higher, but at this stage we are most interested in the qualitative observation that the three burst parameters we calculated are consistent from patch to patch and that they are not affected by increasing pressure until individual bursts become too frequent to resolve. Thus, in the SAK channel, as in the chick muscle channel, it is not the fast kinetic processes or the bursts to which they give rise that are acted on by membrane tension. In both channel types, it is the lifetime of the longest-lived of three closed states – a state which separates bursts – which decreases with increasing negative pressure.

A further similarity between the SAK channel and the stretch-sensitive chick channel is their low and apparently homogeneous membrane density. The density of, for example, Na$^+$ channels ranges from about 100 μm^{-2} in *Myxicola* axons to 3000 μm^{-2} in frog node of Ranvier (reviewed by Hille, 1984). Even at the low end of its range, the Na$^+$ channel has a membrane density about 100 times greater than that of stretch-activated channels. Although we have not made a rigorous study of SAK channel density, the following observations lead us to believe that the distribution is not random and that the channel density is not greater than 1 μm^{-2}. For a randomly distributed, low-density channel, one would expect frequent occurrences of zero-channel and one-channel patches. Instead, small orifice pipettes usually produced two- or three-channel patches (as determined by the number of channels open at high negative pressures), and the larger pipettes about twice as many. Since the areas of our membrane patches were about 8 μm^2 (estimated from patches observed with thin-walled pipette glass), 1 μm^{-2} may overestimate the channel density, but it is probably within a factor of 2 or 3 of being correct. Maintenance of a non-random distribution at low density may be achieved by cytoskeletal elements which limit the lateral diffusive mobility of channels (Almers & Stirling, 1984). These considerations are in keeping with the model presented by Sachs (1986) to explain mechano-transduction by the chick muscle channel.

It is reasonable to question the necessity of postulating a specific transduction mechanism to account for the action of pressure on the SAK channel. Might not changes in mechanical energy act on channel kinetics in a way akin to changes in thermal energy? The fact that only one of the SAK channel's five kinetically distinguishable components is pressure-sensitive argues against this notion. In addition, there are other channel types in the *Lymnaea* heart cell membrane, such as

the low-conductance channel shown in Fig. 1B, which did not show evidence of stretch activation of their gating. Because stretch activation of the SAK channel is observed in excised as well as cell-attached patches, we may rule out another potential non-specific explanation for the stretch-induced increase in P(O), namely that stretch draws up more channel-containing membrane into the patch. At the very least, a 20-fold increase in membrane area would be required to account for observed differences in P(O) as a function of negative pressure. This is patently impossible for an excised patch.

Although a physiological role for SAK channels has yet to be identified, we have hypothesized that they may participate in osmoregulation (Brezden *et al.* 1986). If this is the case, the channels would not be expected to be found exclusively in muscle cells. We have recently found that *Lymnaea* neurones have stretch-activated ion channels with a conductance of 32 pS in normal saline (C. Morris & E. Bédard, unpublished observation). The channels reverse at the resting potential and show a +35 mV shift in their reversal potential when 30 mmol l^{-1} K$^+$ is substituted for normal saline in the pipette. This channel, as does a similar one found in cells isolated from *Lymnaea* kidney, almost certainly has affinities with the SAK channel. Preliminary investigations of volume regulation of *Lymnaea* kidney cells subjected to anisosmotic perturbations show that a quinidine-sensitive pathway limits cell swelling (C. Morris & H. Blois, unpublished observation). Since quinidine blocks SAK channels (Brezden *et al.* 1986), this seems a promising direction for further investigation.

REFERENCES

ALMERS, W. & STIRLING, C. (1984). Distribution of transport proteins over animal cell membranes. *J. Membr. Biol.* **77**, 169–186.
BREHM, P., KIDOKORO, Y. & MOODY-CORBETT, F. (1984). Acetylcholine receptor channel properties during development of *Xenopus* muscle cells in culture. *J. Physiol., Lond.* **357**, 203–217.
BREZDEN, B. L. & GARDNER, D. R. (1984). The ionic basis of the resting potential in a cross-striated muscle of the aquatic snail *Lymnaea stagnalis*. *J. exp. Biol.* **108**, 305–314.
BREZDEN, B. L., GARDNER, D. R. & MORRIS, C. E. (1986). A potassium-selective channel in isolated *Lymnaea stagnalis* heart muscle cells. *J. exp. Biol.* **123**, 175–189.
COLQUHOUN, D. & HAWKES, A. G. (1982). On the stochastic properties of bursts of single ion channel openings and of clusters of bursts. *Phil. Trans. R. Soc. Ser.* B **300**, 1–59.
COLQUHOUN, D. & SAKMANN, B. (1985). Fast events in single-channel currents activated by acetylcholine and its analogues at the frog muscle end-plate. *J. Physiol., Lond.* **369**, 501–557.
COLQUHOUN, D. & SIGWORTH, F. (1983). Fitting and statistical analysis of single-channel records. In *Single-channel Recording* (ed. B Sakmann & E. Neher), pp. 191–263. New York: Plenum Press.
COOPER, K. E., TANG, J. M., RAE, J. L. & EISENBERG, R. S. (1986). Cat-50: A cation-selective channel from frog lens epithelium. *Biophys. J.* **49**, 6a.

ECKERT, R. (1972). Bioelectric control of ciliary activity. *Science* **176**, 473–481.

GELETYUK, V. I. & KAZACHENKO, V. N. (1985). Single Cl⁻ channels in molluscan neurones: multiplicity of conductance states. *J. Membr. Biol.* **86**, 9–15.

GILLES, R. (1983). Volume maintenance and regulation in animal cells: some features and trends. *Molec. Physiol.* **4**, 3–16.

GRINSTEIN, S., DUPRE, A. & ROTHSTEIN, A. (1982). Volume regulation by human lymphocytes. Role of calcium. *J. gen. Physiol.* **79**, 849–868.

GRINSTEIN, S., ROTHSTEIN, A., SARKADI, B. & GELFAND, E. W. (1984). Responses of lymphocytes to anisotonic media: volume-regulating behavior. *Am. J. Physiol.* **246**, C204–C215.

GUHARAY, F. & SACHS, F. (1984). Stretch-activated single ion channel currents in tissue-cultured embryonic chick skeletal muscle. *J. Physiol., Lond.* **352**, 685–701.

GUHARAY, F. & SACHS, F. (1985). Mechanotransducer ion channels in chick skeletal muscle: the effects of extracellular pH. *J. Physiol., Lond.* **363**, 119–134.

HAMILL, O. P. (1983). Potassium and chloride channels in red blood cells. In *Single-channel Recording* (ed. B. Sakmann & E. Neher), pp. 451–471. New York: Plenum Press.

HAMILL, O. P., MARTY, A., NEHER, E., SAKMANN, B. & SIGWORTH, F. J. (1981). Improved patch-clamp techniques for high-resolution current recording from cells and cell-free membrane patches. *Pflügers Arch. ges. Physiol.* **391**, 85–100.

HILLE, B. (1984). *Ionic Channels of Excitable Membranes*. Town, MA: Sinaeur Assoc. Inc.

HUDSPETH, A. J. (1983). Mechanoelectrical transduction by hair cells in the acousticolateralis sensory system. *A. Rev. Neurosci.* **6**, 187–215.

HUGUES, M., SCHMID, H., ROMEY, G., DUVAL, D., FRELIN, C. & LAZDUNSKI, M. (1982). The Ca^{2+}-dependent slow K^+ conductance in cultured rat muscle cells: characterization with apamin. *EMBO J.* **1**, 1039–1042.

LATORRE, R. & MILLER, C. (1983). Conduction and selectivity in potassium channels. *J. Membr. Biol.* **71**, 11–30.

MAGLEBY, K. L. & PALLOTTA, B. S. (1982). Burst kinetics of single channel calcium-activated potassium channels in cultured rat muscle. *J. Physiol., Lond.* **344**, 605–623.

SACHS, F. (1986). Biophysics of mechanoreception. *Membr. Biochem.* (in press).

SARKADI, B., MACK, E. & ROTHSTEIN, A. (1984). Ionic events during the volume response of human peripheral blood lymphocytes to hypotonic media. I. Distinction between volume-activated Cl⁻ and K^+ conductance pathways. *J. gen. Physiol.* **83**, 497–512.

SCHREINER, W., KRAMER, M., KRISCHER, S. & LANGSAM, Y. (1985). Nonlinear least-squares fitting. *PC Tech. J.* **3**, 170–190.

TREHERNE, J. E. (1980). Neuronal adaptations to osmotic and ionic stress. *Comp. Biochem. Physiol.* **67B**, 455–463.

YELLEN, G. (1982). Single Ca^{2+}-activated non-selective cation channels in neuroblastoma. *Nature, Lond.* **296**, 357–359.